Pergamon

PII: S0191-8141(96)00086-7

Journal of Structural Geology, Vol. 19, No. 2, pp. 159 to 170, 1997

0191-8141/97 $17.00 + 0.00

Slickenside and fault surface kinematic indicators on active normal faults of the Alpine Betic cordilleras, Granada, southern Spain

MIGUEL DOBLAS, VICENTE MAHECHA, MANUEL HOYOS and JOSÉ LÓPEZ-RUIZ

Museo Nacional de Ciencias Naturales, Consejo Superior de Investigaciones Científicas, José Gutierrez Abascal 2, 28006 Madrid, Spain

(*Received* 19 *January* 1996; *accepted in revised form* 1 *October* 1996)

Abstract—Twenty four mesoscopic slickenside kinematic indicators are described here for the Pliocene–Quaternary active normal faults of the Alpine Betic Cordilleras, Granada, southern Spain. The indicators are classified into twelve groups depending on the down- or up-slope asymmetric orientation of features such as concavities, damaged versus sharp grain-borders or step-edges, V-shaped markings, fractures, and trailed material.

Seventeen of the indicators were not previously described in the literature. The new kinematic indicators include two types of asymmetric grains, a carrot-shaped marking, six substructures of congruous and incongruous steps, trailed fault material, a drop-shaped figure, a V-shaped marking, three types of synthetic hybrid fractures with congruous steps, and two varieties of pluck holes. We think that some of these kinematic indicators provide information on the amount of displacement, aseismic versus seismic slip rates, cataclastic flow, frictional wear, or surface polishing. © 1997 Elsevier Science Ltd. All rights reserved

INTRODUCTION

The deduction of the sense of movement on a fault plane using slickenside features has been a common procedure in structural geology for many years. The most recent attempts to classify the classical brittle or *sensu stricto* (Will and Wilson, 1989) slickenside kinematic criteria have been undertaken by Petit *et al.* (1983), Doblas (1985, 1987), Petit (1987), Mercier and Vergely (1992), and Angelier (1994). Several authors have suggested the existence of other types of slickensides (most of them non-brittle): (1) *sensu lato* (Will and Wilson, 1989), hot (Lister and Davis, 1989), or *ridge-in-groove* (Means, 1987) slickensides found on the *C* planes of ductile *S–C* tectonites (Doblas, 1985, 1987, 1991; Wilson and Will, 1990; Lin and Williams, 1992); (2) slickensides related to the flow of magma (Nichols, 1938; Smith, 1968; Doblas *et al.*, 1988; Pierce *et al.*, 1991); (3) hydroplastic slickensides due to faulting in incompletely lithified sediments (Guiraud and Séguret, 1987; Petit and Laville, 1987); (4) pedogenic slickensides (Gray and Nickelsen, 1989); (5) antropic slickensides formed during the mechanical excavation of rock (Spray, 1989); and (6) microscopic slickensides with different types depending on the presence of a coating and/or a deformed host layer (Lee, 1991).

Few studies have analyzed slickenside kinematic indicators on active faults. The only such study was by Hancock and Barka (1987) along a normal fault scarp in Turkey artificially exhumed by engineering work. These authors suggested four shear sense criteria as typical of slickensides in shallow active normal faults. Other studies analysing kinematic indicators in active normal faults were done in the Aegean region (Stewart and Hancock, 1991), and in the U.S. and Mexican Basin and Range provinces (Power and Tullis, 1989; Suter *et al.*, 1995).

In the present study, we intend to provide a field guide for slickenside kinematic studies, presenting twenty four indicators including seventeen new ones (Fig. 1). It seems that even after half a century of detailed kinematic analyses of slickenside indicators, more criteria remain to be discovered. According to Means (1987) "With seismological and tectonic interest in fault rocks increasing, the time seems ripe for a new wave of research on the structure and significance of slickensides."

SLICKENSIDE KINEMATIC INDICATORS IN THE ACTIVE NORMAL FAULTS OF SOUTHERN SPAIN

Tectonic setting

The study area is located in the Granada province, southern Spain and it belongs to the Betic Cordilleras, the westernmost branch of the Alpine Mediterranean orogenic system (Fig. 2). The Cordilleras have been subdivided into an Internal Zone and an External Zone based on structural and paleogeographic criteria (Fig. 2). The Internal Zone contains three main units (Torres-Roldán, 1979). From oldest to youngest these are: Nevado-Filábride, Alpujarride and Maláguide. The orogenic edifice resulted from late Cretaceous to early Miocene compressional tectonics, overprinted by Neogene extensional detachments, and Neogene to Quaternary high- to medium-angle normal faulting (Doblas and Oyarzun, 1989a,b).

We analyze three exhumed normal fault zones that belong to the Alpujarride Unit of the Internal Zone (Figs 2 & 3): the Padúl–Nigüelas fault zone (PNFZ), the Cázulas fault (CF), and the Frigiliana fault zone (FFZ). These normal faults display nearly 40 km of fault-front,

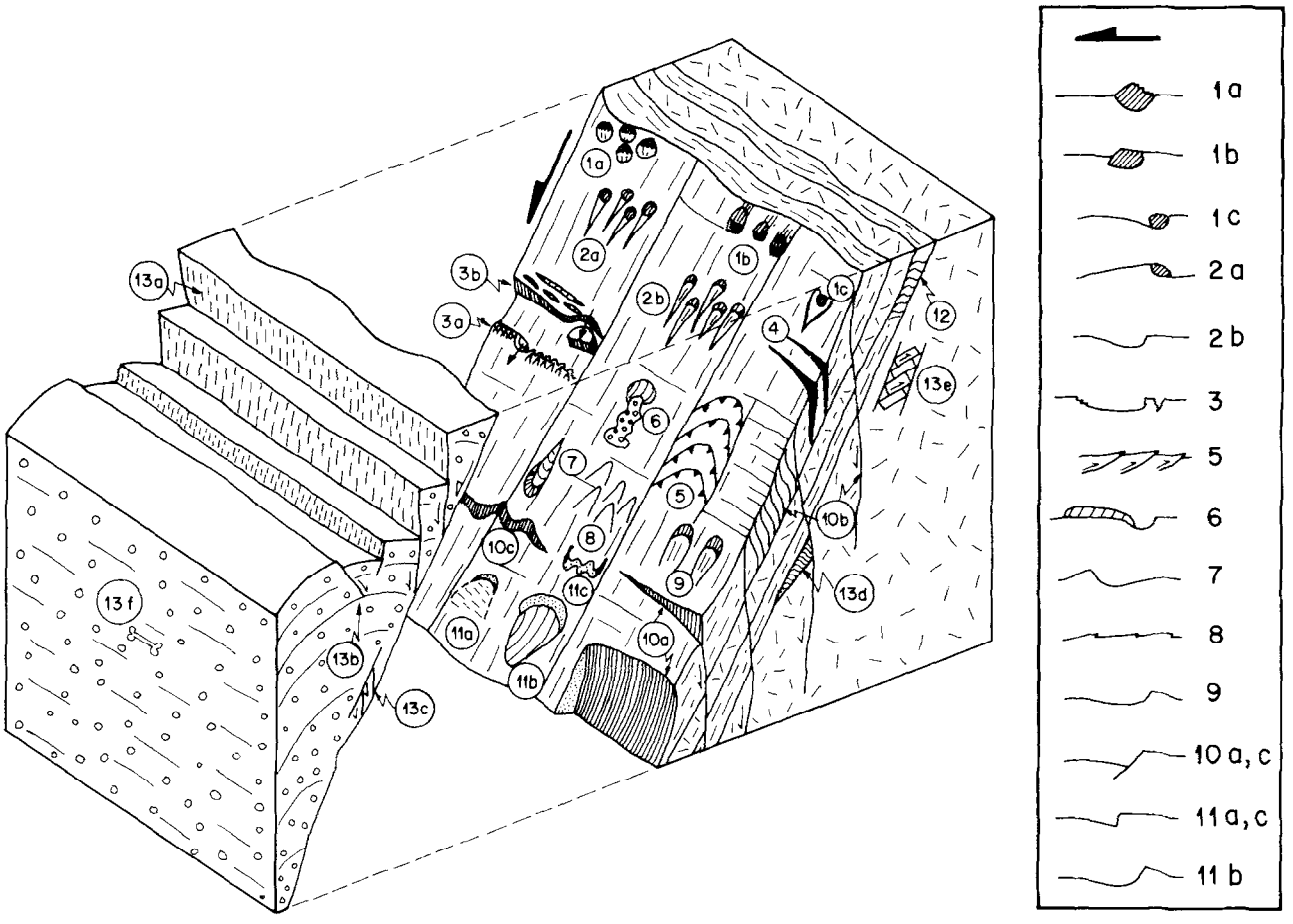

Fig. 1. Schematic block-diagram depicting the various kinematic indicators found on the normal faults of Granada. 1. Asymmetric grains; 2. Carrot-shaped markings; 3. Substructures of congruous and incongruous steps; 4. Tension gashes; 5. Crescentic comb/reverse fractures; 6. Trailed fault material; 7. Drop-shaped features with frontal push-up microridges; 8. V-shaped markings; 9. Concave-shaped congruous pluck steps; 10. Synthetic hybrid fractures; 11. Pluck holes and spall marks; 12. Congruous drag-effect on a previously planar element; 13. Kinematic indicators outside the fault planes. Inset shows the geometry of some of the indicators in cross-sections orthogonal to the fault surface and parallel to the striations. The indicators not represented in this inset are already shown in cross-section in the block diagram.

up to 60 scarps, and approximately 4 km^2 of outcropping slip surfaces (Fig. 3). These fault scarps are up to 300 m in height and dip angles range between 30° and 80°. Locally, these faults show strike-slip components and multiple sets of striae. However, we avoided these components in our study, and analyzed only the 'pure' normal fault surfaces. The normal sense of throw is corroborated by up to 100 m of Middle Pleistocene to Holocene detrital-lacustrine deposits which are found in the deepest fault border of the Lecrín half-graben. Similarly, the CF and FFZ bound tens of meters of Upper Pleistocene to Holocene alluvial fan deposits (Hoyos, 1992). Many fault-plane geometries exist: mirror-like planar, irregular, corrugated, listric, etc. The 'stratigraphy' of the slickenside planes (Means, 1993) is also highly complex with various coatings and/or deformed wall-rocks.

The Padúl–Nigüelas fault zone (PNFZ; Fig. 3a–d) trends NW–SE to WNW–ESE, and dips 30°–50° toward the southwest to south-southwest. This fault zone bounds the Pliocene–Quaternary Lecrín half-graben to the southwest, where the active sector of this fault zone shows spectacular fault scarps, triangular faceted spurs, and alluvial fans (Doblas *et al.*, 1993, 1995). It develops on the Alpujarride unit near its eastern contact with the Nevado-Filabride extensional-related metamorphic core-complex (Doblas and Oyarzun, 1989a). The rocks are brecciated Triassic marbles, limestones, dolomites, other undifferentiated Paleozoic metamorphic rocks, and Pliocene–Quaternary detrital sediments. The Cázulas fault (CF; Fig. 3e) and the Frigiliana fault zone (FFZ; Fig. 3f) are WNW–ESE-oriented normal faults (dipping 40°–80° to the south-southwest; Fig. 2) outcropping in two areas to the southwest of Granada, and affecting Cambrian and Permo-Triassic brecciated marbles, mica schists, and quartzites, as well as Pliocene–Quaternary sediments. The PNFZ, the CF and the FFZ belong to a regional trend of seismically active faults (IGN, 1992; Doblas *et al.*, 1993).

Slickenside observations

We have found 24 slickenside kinematic indicators in the active normal fault zones of southern Spain and

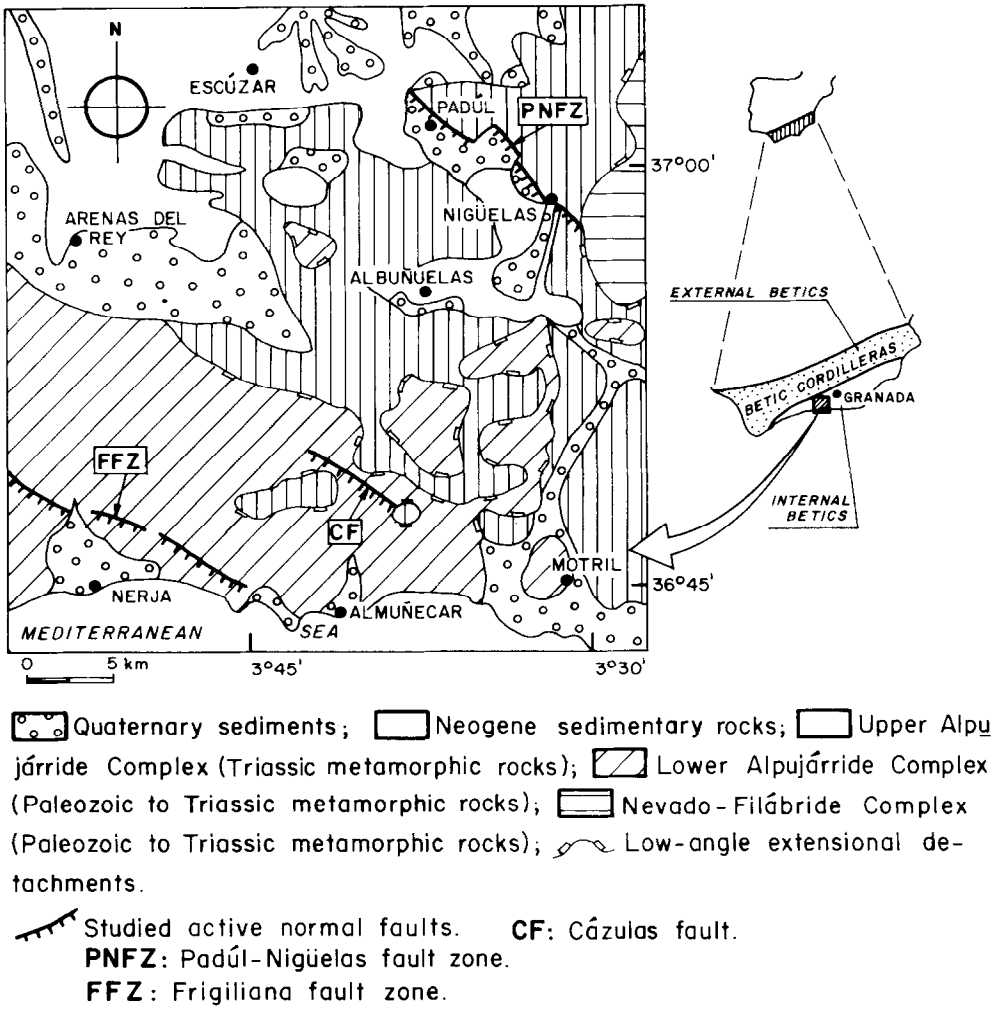

Fig. 2. Simplified geologic map of the studied area in the Betic cordilleras, Granada, southern Spain (modified from IGME, 1973).

separated them into 12 groups. Seventeen of these indicators are new to the slickenside literature. In this section we describe all these indicators which are identified with their corresponding letters and numbers on Fig. 1. As the faults are dip-slip normal faults we refer to the sense of shear in relation to the down-slope or up-slope asymmetric orientation of specific geometric features of the indicators (concavities, V-shaped markings, damaged versus sharp grain-borders or step-edges, fractures, and trailed material), which are pointing toward the sense of movement of the hangingwall (down-slope), or the opposite (up-slope). We identified each criteria several times on different fault surfaces of the study area, and thus we consider that they are reliable kinematic indicators. In the following paragraphs we will present the twelve groups of indicators found on the fault surfaces, and an additional group of indicators observed outside the slickenside planes.

Asymmetric grains. Several asymmetric features associated with protruding grains can be used as kinematic indicators. Three types of asymmetric grains are observed (1 in Fig. 1). Their dimensions range between 1 and 10 cm.

The first one, not previously described (1a in Fig. 1), is constituted by asymmetric grains displaying damaged or bruised frontal sectors which are pointing up-slope (opposite to the movement of the hangingwall; Fig. 4a–e).

The second one (1b in Fig. 1) consists of asymmetric grains with polished lee sectors pointing up-slope (Fig. 4f). This indicator ressembles the *slickensided roches moutonnées* of Tjia (1967), and the *knobby elevations* of Dzulynski and Kotlarczyk (1965). However, the present indicator develops on an individual grain, while knobby elevations may develop on any irregularity of the fault surface. The indicators 1a and 1b result from differential wearing and polishing acting on the up-slope sectors of the protruding grains, and they represent contraction-related features equivalent to some of the features that we describe later in incongruous steps.

The third indicator (1c in Fig. 1) consists of *spoon-shaped depressions* (Power and Tullis, 1989) surrounding isolated/protruding grains or other irregularities (Fig. 4g).

Carrot-shaped markings. Two types of carrot-shaped markings are present with lengths ranging between 0.5 and 5 cm (2 in Fig. 1).

Sheltering markings with gouge trails (2a in Fig. 1) are found behind protruding grains with angles opening up-slope (against the sense of movement of the hangingwall; Fig. 4h). This indicator is similar to the *trails* of Willis and Willis (1934) and Tjia (1967, 1968), the *oval steps* of Gay (1970), the sheltered gouge *trails* of Power and Tullis (1989), or the *scour marks* on loose materials such as sand or snow (Allen, 1965).

The second indicator (2b in Fig. 1) consists of gouge markings with angles oriented as in the previous case (opening up-slope), and resulting from the gouging effect of protruding grains which have been plucked away (Fig. 4i). This indicator 2b is opposite to the classical *gouging-grain grooves* or *prod marks* (Willis and Willis, 1934; Tjia, 1967, 1968; Jackson and Dunn, 1974; Spray, 1989) usually observed at the mm- or microscopic-scale (Engelder, 1974), and which are characterized by carrot-shaped marks with angles opening down-slope (these marks correspond to grains stuck against irregularities of the fault surface). However, our second case ressembles the *niches d'arrachement* of Vialon *et al.* (1976), as they both display spoon-shaped congruous microsteps whose risers are facing down-slope. However, they are different in that the *niches d'arrachement* do not show carrot-shaped markings.

Substructures of congruous and incongruous steps. We found six different substructures in two types of steps (congruous and incongruous; 3 in Fig. 1). Congruous steps show risers facing in the same direction as the movement of the hangingwall (down-slope), and the reverse happens with incongruous steps (Norris and Barron, 1969). Both might also be defined as the *positive smoothness criterion* and the *negative smoothness criterion*, respectively (Angelier, 1994). However, the distinction between congruous and incongruous steps has always been difficult and controversial (14 different types of steps are known; Doblas, 1987). The substructures described here range in size between a few mm and 1 m, they all are new in the literature, and they might be the most useful features to identify correctly congruous and incongruous steps. The steps are generally of the fracture or plucking type.

Incongruous steps (3a in Fig. 1) usually show contraction-related features in their borders pointing up-slope, such as mm-scale microarrow-shaped polished indentations (*IS* in Fig. 5a), damaged or bruised sectors (Fig. 5b & c), or microflakes thrusted down-slope (asterisks in Fig. 5b).

In contrast, congruous steps (3b in Fig. 1) show tension-related structures in their borders pointing down-slope such as sharp edges (up to 1 m) with tension fractures (*CS* in Fig. 5a) or detached fragments (Fig. 5d). These congruous detached fragments are opposite to the *stick-slip spalling* criterion of Riecker (1965) and Tjia (1967, 1968).

To our best knowledge, the only studies to analyze substructures of fault steps were by Guiraud and Séguret (1987) who studied hydroplastic slickensides characterized by incongruous *push-up pressure microridges*, and by Lin and Williams (1992) who described *rough congruous steps* and *smooth incongruous steps* in ridge-in-groove-type slickensides in *SC* ductile tectonites. Other authors have described contraction-related features associated with more localized grains or fragments (not specifically steps): *slickolites* (Arthaud and Mattauer, 1969), *P* or *rs planes* (Petit *et al.*, 1983; Petit, 1987), V-shaped figures and indented/festooned slab edges (Bossière and Sellier, 1993; Sellier and Bossière, 1993).

The substructures of congruous and incongruous steps presented here are in accordance with the well-known smoothness/roughness criterion of Billings (1942). However, as widely discussed in the literature, kinematic inferences based only on the 'hand rule' of Billings (1942) are unreliable.

Tension gashes. Tension gashes are abundant in the studied faults. They trend subperpendicular to the direction of the striae on the slickenside planes (4 in Fig. 1), and they penetrate the fault surface dipping 45° down-slope. Their dimensions range from a few cm to 1 m. Tension gashes have been commonly used as kinematic indicators in slickensides (Dzulynski and Kotlarczyk, 1965; Tjia, 1967; Norris and Barron, 1969; Petit, 1987).

Crescentic comb/reverse fractures. These reverse fractures show crescentic geometries with concavities oriented downslope (5 in Figs 1 & 5e), while their inclination and antithetic sense of movement is opposite (up-slope). Their dimensions are generally between 15 and 50 cm. They display high angles with respect to the plane of the faults, and might be interpreted as comb, transverse tensile, or tear fractures, or pinnate joints (Hancock, 1985; Suppe, 1985; Hancock and Barka, 1987; Spray, 1989). According to Hancock and Barka (1987), comb fractures are common along high-angle normal faults. The indicator shown in Fig. 5(e) displays the same concavities as the *crescentic fractures* of Harris (1943), the *lunate friction cracks* of Wardlaw *et al.* (1969), or the

Fig. 3. General views of the studied normal faults. (a) Aerial view of the fault front in the southern sector of the Padúl–Nigüelas normal fault zone (PNFZ; the image is 4 km across; photograph taken by Florencio Aldaya). (b) Fault front in the southern sector of the PNFZ (width of the photograph: 1 km). (c) Fault front in the central sector of the PNFZ (width of the photograph: 2 km). Note the fault scarps, triangular faceted spurs and alluvial fans in these three photographs of the PNFZ. (d) Detail of a fault scarp in the PNFZ (the photograph is 40 m across). (e) Fault scarp along the Cázulas normal fault (width of the photograph: 20 m). (f) Fault surface in the Frigiliana fault zone (the photograph is 40 m across, and the approximate height of the cliff is 100 m).

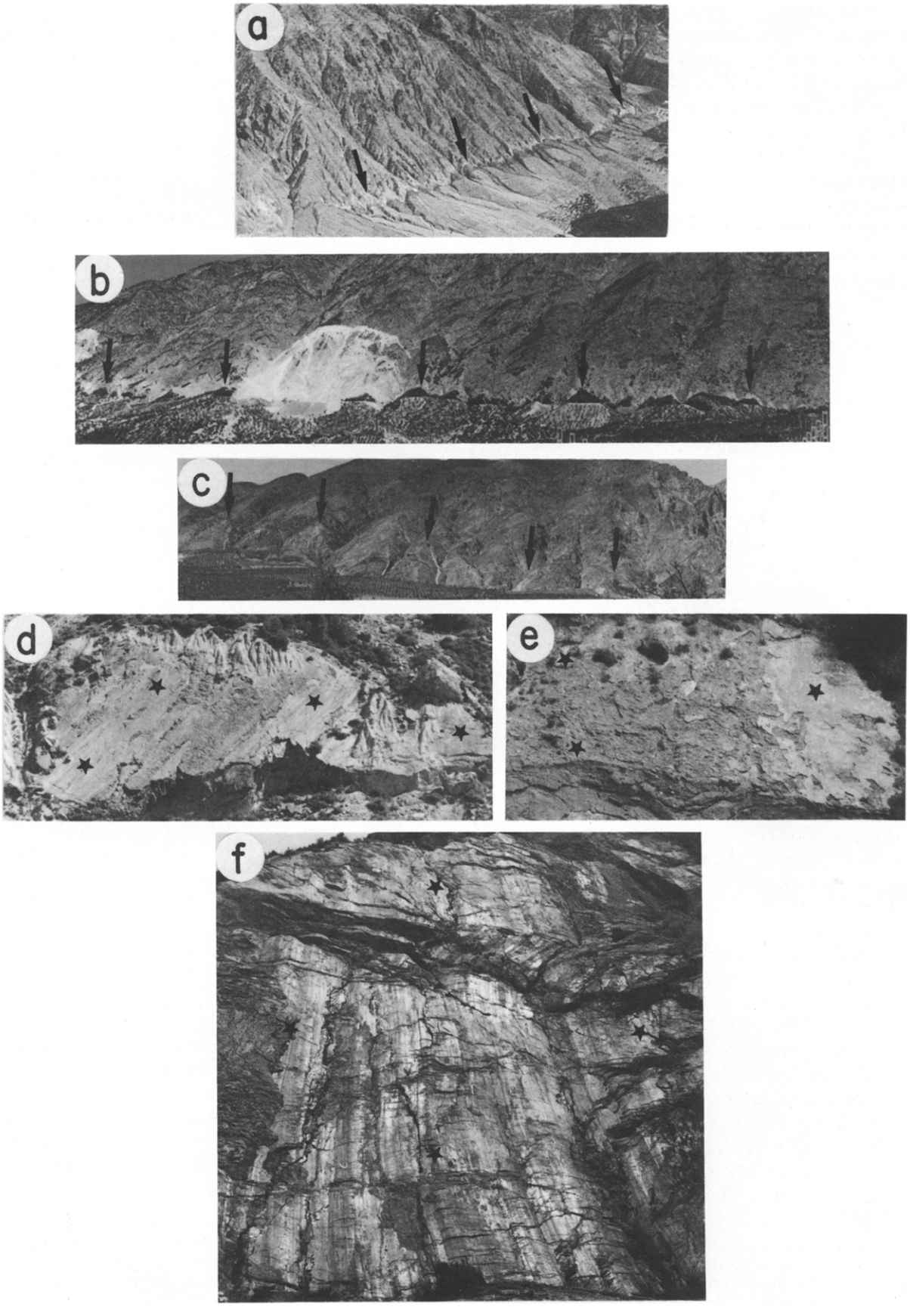

Fig. 3.

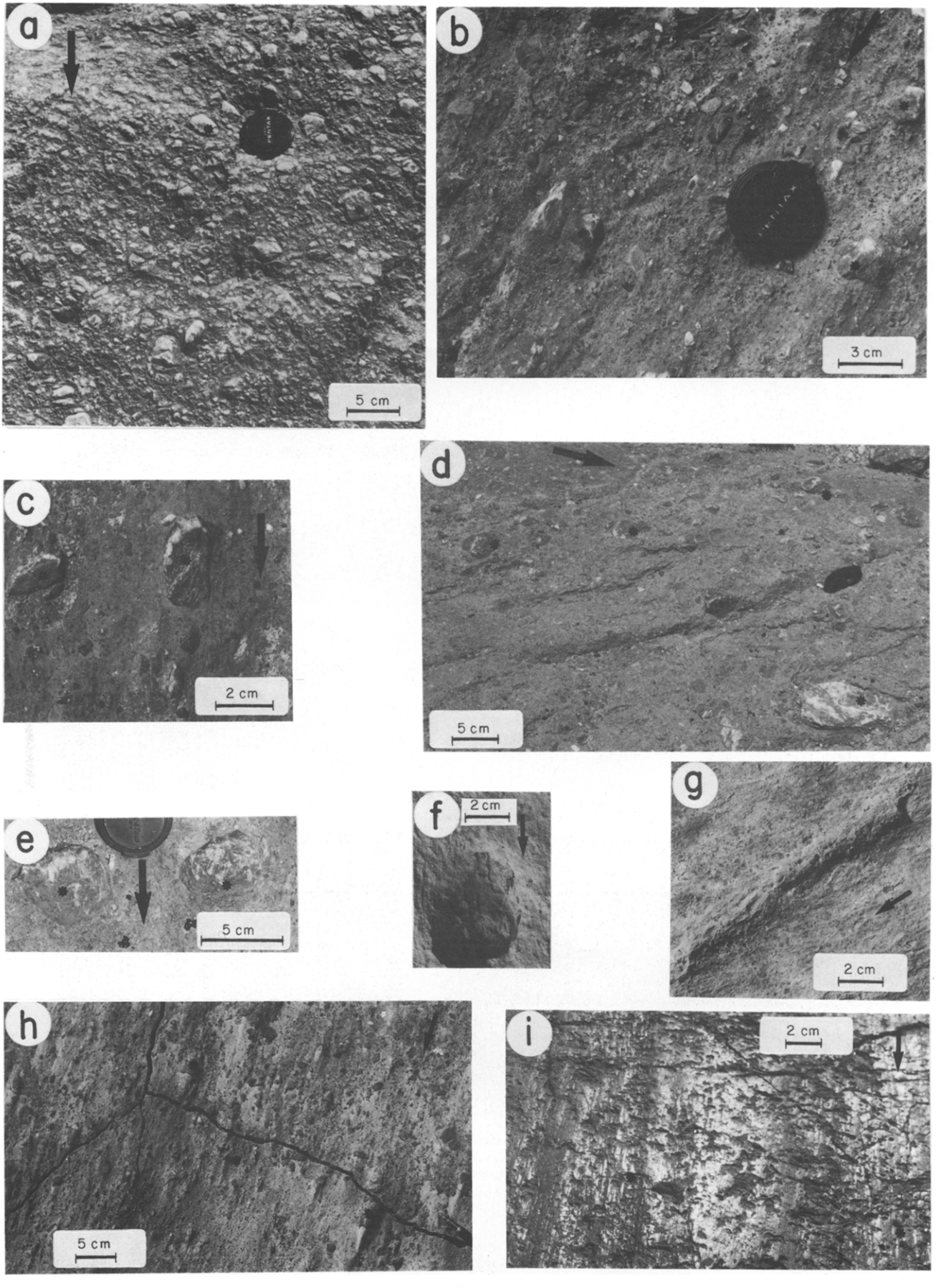

Fig. 4.

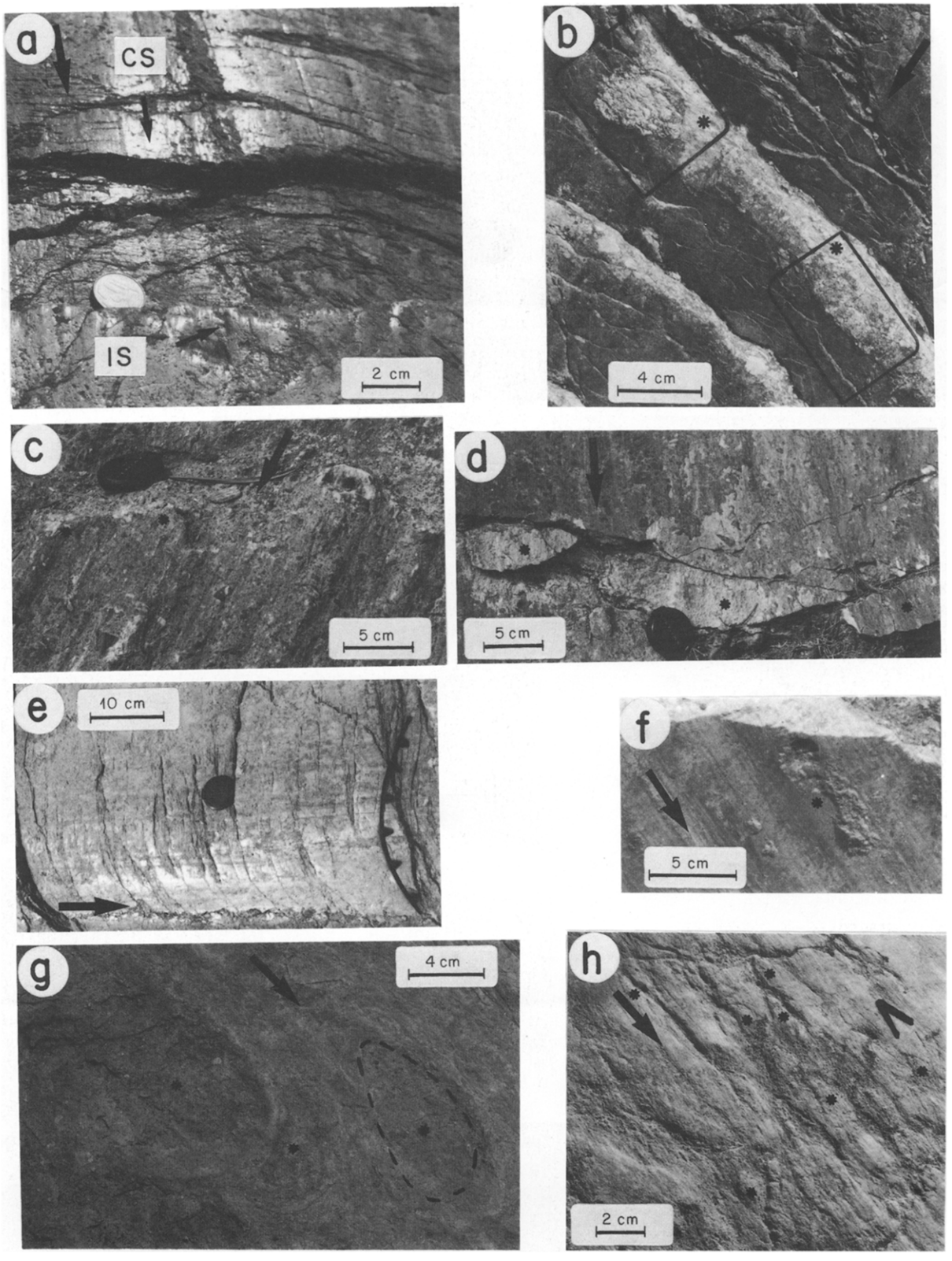

Fig. 5. Examples of slickenside kinematic indicators on the studied faults. (a,b,c and d) Substructures of congruous and incongruous steps. (e) Crescentic comb/reverse fractures. (f) Trailed fault material. (g) Drop-shaped figures with frontal push-up microridges. (h) V-shaped markings. The arrows indicate the down-slope sense of movement of the hangingwall. Asterisks locate some of the indicators.

Fig. 4. Examples of slickenside kinematic indicators on the studied faults. (a,b,c,d and e) Asymmetric grains with damaged or bruised frontal sectors. (f) Asymmetric grain with a polished lee sector. (g) Spoon-shaped depression. (h) Carrot-shaped sheltering markings with gouge trails. (i) Carrot-shaped gouge markings. The arrows indicate the down-slope sense of movement of the hangingwall. Asterisks locate some of the indicators.

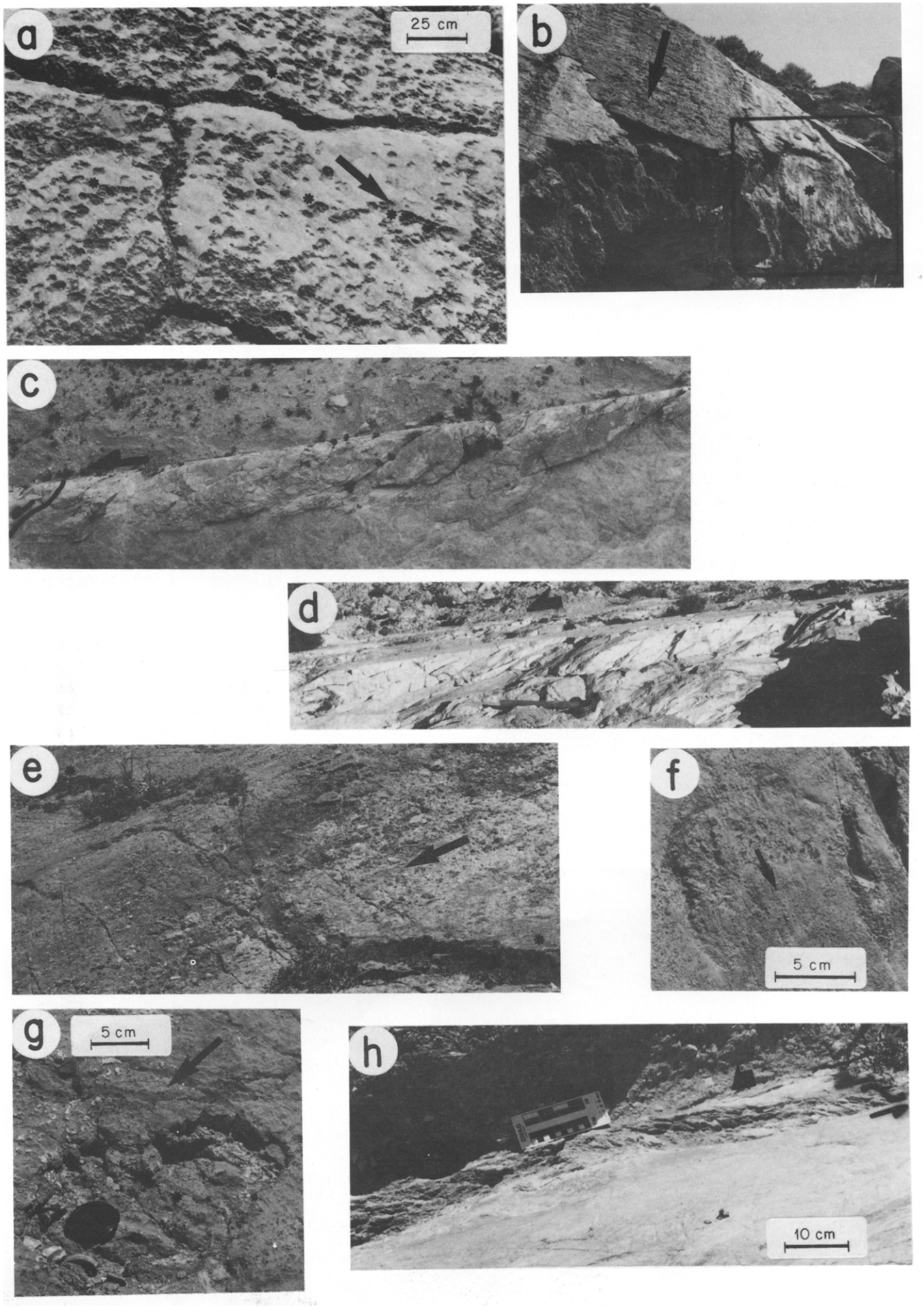
a
25 cm
b
c
d
e
f
5 cm
g
5 cm
h
10 cm

parabolic marks of Angelier (1994), but the opposite concavity to the one suggested by Hancock and Barka (1987) for comb fractures; the latter are similar to the *crescentic gouge* of Willis and Willis (1934), and the *curved pinnate secondary shears* of Tjia (1967).

Trailed fault material. Loose fault material is occasionally trailed down-slope and plastered away from its original area (6 in Figs 1 & 5f). The dimensions of these structures range between 5 and 25 cm. This 'plastic-like' criterion is probably indicative of cataclastic flow (Rutter, 1993). To our best knowledge, no kinematic indicator of such a kind has been described.

Drop-shaped figures with frontal push-up microridges. These drop-shaped figures have their widest parts with push-up microridges oriented down-slope (7 in Figs 1 & 5g). They are somewhat similar to the *grooves* of Tjia (1967, 1968), with a difference in scale (the ones described here are larger, i.e. 10 to 30 cm long) and also in that our indicators show frontal push-up microridges. These markings are probably formed by rigid objects being slowly sheared down-slope while being pressed against the fault planes. This case is similar to the cavities described by Suter *et al.* (1995) in some faults. However, these last symmetric features have been related to non-slip behaviour on the fault planes (Suter *et al.*, 1995), while our asymmetric criterion indicates active slip along the fault planes.

V-shaped markings. A series of V-shaped markings are observed, with angles opening downwards in the direction of movement of the hangingwall. These indicators are different from the carrot-shaped markings described previously in that the former are much larger features (sizes range between 2 and 5 cm), and they are not related to isolated grains (they are directly carved on the brecciated fault surface). The present indicators probably result from sheltering effect on local irregularities (e.g. the intersection of planar elements penetrating the fault surfaces or the existence of protuberances; 8 in Figs 1 & 5h). A similar case corresponds to the *triangular patches of gouge* of Norris and Barron (1969). However, in our case we are not dealing with gouge but with a brecciated fault surface.

Concave-shaped congruous pluck steps. These figures are characterized by spoon-shaped congruous microsteps (2–5 cm) with concavities oriented down-slope, resulting from the plucking and gouging effect of grains torn away from their initial locations (9 in Figs 1 & 6a). These features resemble the *niches d'arrachement* proposed by Vialon *et al.* (1976). However, in their study, no examples of these structures were provided — the features were only theoretically described.

Synthetic hybrid fractures. These fractures that are common in the study area (10 in Fig. 1) were not described previously. Their dimensions range between 0.5 and 50 m. They display angles between 30° and 50° to the fault plane and are not *R* Riedel fractures, which have angles between 10° and 20° (Hancock, 1985). They are synthetic and inclined downwards, and they are probably related to the *hybrid fractures* of Hancock (1985). The present synthetic hybrid fractures differ from the comb fractures described by Hancock and Barka (1987) in that the angles of the former with the fault plane are smaller, their displacements are greater (cm to m), they show well striated planes, and they are synthetic.

Three different indicators are associated with synthetic hybrid fractures.

The first case consists of meter-scale spoon-shaped synthetic hybrid fractures (10a in Fig. 1) that are typically found in the lower exhumed sectors of the normal faults (Fig. 6b), and might be related to fault-termination splay fractures (Mercier and Vergely, 1992), step-down zones (Stewart and Hancock, 1991), or secondary extensional faults nearby a locking area on the main normal fault (Dunne and Hancock, 1994).

The second indicator is characterized by trains of sigmoid en échelon synthetic hybrid fractures (10b in Fig. 1), which are found in sections orthogonal to the fault planes and parallel to the striae, either transecting a wide section of fault slip-plane and brecciated bedrock (this is the largest kinematic indicator found in our faults, i.e. 10 m up to 50 m; Fig. 6c), or only the slickenside plane (50 cm to 1 m; Fig. 6d). The orientation of these trains of fractures closely resembles the sigmoid patterns of en échelon tension gashes or fractures.

The third indicator consists of synthetic hybrid fractures with sinuous traces on the fault plane (10c in Figs 1 & 6e).

One might wonder if these synthetic hybrid fractures are late, independent faults, or if they are coeval with the movement of the main normal fault. Several arguments support the latter hypothesis: (1) synthetic hybrid fractures show slickenside lineations, with orientations similar to the major fault plane; (2) synthetic hybrid fractures often splay progressively off the main fault plane, and no clear cross-cutting relations were observed; (3) the trains of sigmoid faults most probably represent coeval en échelon secondary features; and (4) the spoon-shaped geometries are always restricted to the major fault

Fig. 6. Examples of slickenside kinematic indicators on the studied faults. (a) Concave-shaped congruous pluck steps. (b) Meter-scale spoon-shaped synthetic hybrid fractures (width of the photograph: 11 m). (c and d) Trains of sigmoid en échelon synthetic hybrid fractures; the fault planes actually dip 45° to the left; the two photographs are 70 and 22 m across, respectively. (e) Sinuous synthetic hybrid fracture (width of the photograph: 3 m). (f) Down-slope concave pluck hole. (g) Pluck hole with congruous step and plastered material down-slope. (h) Congruous drag-effect on a previously planar element (bedding S_o). The arrows indicate the down-slope sense of movement of the hangingwall. Asterisks locate some of the indicators.

plane, and they are never found outside this zone (neither on the fault plane nor on a cross-section).

Pluck holes and spall marks. Three types of pluck holes and spall marks ranging in size from 10 to 30 cm are found.

The first indicator consists of concave pluck holes (11a in Fig. 1), that represent incomplete plucking of fault material (Fig. 6f). In this case the kinematic indicator derives from the down-slope orientation of the concavity, similarly to the *croissants concaves* of Petit *et al.* (1983). The features described by the last authors were accompanied by synthetic fractures in the steep sides, and these fractures are missing in our examples.

The second indicator is characterized by pluck holes with congruous steps in their upper parts (11b in Figs 1 & 6g). The example depicted in Fig. 6(g) also shows trailed fault material which has been dragged and plastered toward the down-slope sector of the pluck hole. Pluck holes were described in similar active normal faults by Hancock and Barka (1987). These authors did not use these structures as kinematic indicators, but they described somewhat similar features which they called *asymmetric depressions*, characterized by short steep sides facing up-slope. This indicator is opposite to the one described in our paper which shows congruous steps.

The last indicator consists of spall-marks (11c in Fig. 1), which also show congruous steps in their upper parts. This criterion is similar to the one suggested by Hancock and Barka (1987).

Congruous drag effect. The drag effect on previously planar elements is a well known indicator in fault zones. In some of the studied normal faults, the initial S_o bedding surfaces of the rock are dragged congruously down-slope, giving them an *S*-shaped geometry inclined towards the sense of movement of the hangingwall (12 in Figs 1 & 6h). The dimensions of these structures range between 5 cm and 1 m. This criterion is similar to the *gradins de feuilletage* of Vialon *et al.* (1976), or the *bending effect* of Lee (1991).

Other kinematic indicators not on the slickenside planes. Apart from the slickenside kinematic indicators described previously, six other shear sense criteria have been observed outside the fault planes (13 in Fig. 1): mesoscopic folds and faults in the Pliocene–Quaternary detrital sediments (13a & b in Fig. 1); small-scale deformation of the basal Quaternary deposits such as microfaults and asymmetric microfolds (13c in Fig. 1); *SC*-type fault gouges in contact with the slickenside planes (13d in Fig. 1); domino-type block faulting in sections perpendicular to the fault planes along the direction of movement (13e in Fig. 1); and abundant stratigraphic criteria which reinforce the sense of movement deduced for all these normal faults (13f in Fig. 1).

DISCUSSION

The slickensides found in the active normal faults of Granada were probably formed at depths below 1 or 2 km, with ambient temperatures lower than 270°C, as in the cases described by Hancock and Barka (1987) and Power and Tullis (1989). The PNFZ shows a minimum throw during its neotectonic activity of 900 m, which corresponds to the topographic difference between a perched Pliocene–Quaternary paleosurface and the valley bottom.

A characteristic of the neotectonic normal faults in the study area is the presence of structural heterogeneities, with along-strike disruptions such as the ones described by Stewart and Hancock (1991): step-over zones, step-up zones, step-down zones, and cross-faults. These complexities make it difficult to distinguish between faults resulting from contrasted regional-scale episodes (see for example the case described in Turkey by Dumont *et al.*, 1981), and faults resulting from these structural heterogeneities. Thus, the use of stress inversion techniques would seem rather unreliable in this region (as suggested by Pollard *et al.*, 1993). Moreover, this is a seismically active region which displays single fault surfaces with multiple slip vectors which might result from different earthquakes (as proposed in another area by Cashman and Ellis, 1994).

Of the slickenside-related kinematic indicators suggested by Hancock and Barka (1987) for active normal faults (comb fractures, tool tracks, asymmetric cavities, and spall marks), in southern Spain, only spall marks have proven useful. Tool tracks, which are abundant in our study area, show very complex geometries.

Hancock and Barka (1987) proposed that active normal faults are characterized by corrugations which they ascribe to the "...upwards propagation of slip planes seeking undemanding pathways through heterogeneous fault precursor breccias...". However, in Granada we found corrugated, irregular, listric, or perfectly planar fault planes, both in contact with wide precursor breccia zones, or slightly brecciated bedrock. Some fault planes even show contrasted corrugated and mirror-like sectors. These large geometrical variations of the studied normal faults have still to be explained.

The neotectonic normal faults of Granada are particularly prone to what might be called 'pseudocriteria' resulting from 'dip-slip' erosion processes, which are often easily misinterpreted with true tectonic criteria in these young faults, such as 'false' spall marks, gouging grooves, sheltering trails, pluck holes, congruous crystal fibers, trailed fault material, tool tracks, etc.

A major objective in the study of slickensides is the detection of features indicative of seismic or aseismic slip-rates (Spray, 1989; Means, 1993; Tullis, 1993). However, very few structures are unambiguous seismic indicators (Means, 1993). In any case, and according to Power and Tullis (1989) "...the possibility of finding other features which can be directly linked to seismically or geodetically

observed aspects of fault behaviour is great, and should be pursued".

In the active normal faults of southern Spain, rates of slip cycle over time from seismic to aseismic as is the case in most faults (Power and Tullis, 1989; Scholz, 1990). Several indicators which can be attributed to the seismic phase of the earthquake cycle are being investigated in the slickenside planes of the area, such as *jigsaw implosion breccias* (Sibson, 1986), which are particularly abundant in the Frigiliana normal fault zone. The angle of the synthetic hybrid fractures with respect to the normal faults of Granada might be indicative of the temperature or sliding behavior (stable or stick-slip), according to ideas of Moore *et al.* (1989) in similar fractures, and thus may be used as a potential paleoseismic tool. Similar to what happens in tension gashes (Ramsay and Huber, 1987), variations in these angles might also reflect positive or negative dilation along the fault.

In relation to the mechanisms of formation of slickensides (Power and Tullis, 1989), most kinematic indicators in the studied faults were generated either by frictional wear and surface polishing (Hancock and Barka, 1987), or by streaking or trailing of lightly cemented gouge material (Engelder, 1974).

Some of the kinematic criteria found in the present study of normal faults are indicative of mechanisms and conditions of faulting. According to Gay (1970) the predominance of congruous steps would indicate a more advanced stage in the evolution of fault planes (incongruous steps would be typical of small amounts of displacement). Congruous steps are dominant in the normal faults of Granada, in opposition to the suggestion of Hancock (1985) that incongruous steps predominate under frictional-wear conditions. We tentatively suggest that the asymmetric grains and incongruous steps described previously might be indicative somehow of the amount of displacement along the faults: small if they are bruised, and larger if they are polished.

Some morphologically ductile shear sense criteria displayed by the normal faults are indicative of cataclastic flow conditions (Rutter, 1993), during which the material behaves as a loose sand, and grain-boundary sliding occurs between particles entirely within the brittle field (Rutter, 1993). Some of the ductile-looking fabrics include thrusted microflakes in incongruous steps (Fig. 5b), trailed fault material (Fig. 5f), frontal push-up microridges (Fig. 5g), congruous drag-effect (Fig. 6h), plastic-like depressions, and folds. It is probable that these structures are the result of aseismic slip along the faults. Some of the cavities found in these normal faults are strikingly similar to the ones described by Suter *et al.* (1995), which are thought to be the result of indentation phenomena during non-slip periods, and might indicate stick-slip behavior of the faults (Suter *et al.*, 1995).

Some of the kinematic indicators observed in the faults of southern Spain are the direct result of the 'granular' initial rock types (brecciated metamorphics and detrital sediments). These include asymmetric grains, carrot- and V-shaped markings, concave-shaped pluck steps, and some pluck holes and spall marks. Consequently, initially homogeneous rocks (quartzites, limestones, aplites, etc.) would probably give rise to faults mostly devoided of granular wall material.

Not all the slickenside indicators described here on active normal faults will be equally useful for future kinematic analyses. Some of the more widespread and better constrained indicators might be widely used, i.e. asymmetric grains, substructures of congruous and incongruous steps, trailed fault material, etc. In particular, the detailed meso- and microstructural analysis (slickenside petrography; Lee and Means, 1990) of tension- or contraction-related features of congruous and incongruous steps should be a very effective tool. In contrast, some other indicators which are either already known (tension gashes) or less well understood (comb fractures, V-shaped markings, etc.) might have a more restricted use.

Acknowledgements—We are specially grateful to Drs Z. Reches, J. Maghlouglin, and S. Wojtal for useful reviews of this manuscript. We also acknowledge the comments on a previous version of this paper by Drs J. Spray, D. Faulkner, and R. Maddock. We thank José Arroyo for the drafting work. Financial support was provided by the 'Dirección General de Investigación Científica, y Técnica' (DGICYT) of the Spanish 'Ministerio de Educación y Ciencia' through Projects PB-92-0108 and PB-92-0024.

REFERENCES

Allen, J. R. L. (1965) Scour marks in snow. *Journal of Sedimentary Petrology* **35**, 331–338.

Angelier, J. (1994) Fault slip analysis and paleostress reconstruction. In *Continental Deformation*, ed. P. L. Hancock. Pergamon Press, Oxford, 53–100.

Arthaud, F. and Mattauer, M. G. (1969) Exemples de stylolites d'origine téctonique dans le Languedoc; leurs relations avec la téctonique cassante. *Bulletin de la Société geologique de France* **7**, 738–744.

Billings, M. P. (1942) *Structural Geology*. New York, Prentice-Hall.

Bossière, G. and Sellier, D. (1993) Observation d'enduits siliceux et titanés sur des surfaces polies d'origine glaciaire. *Compte rendu de l'Académie des Sciences Paris* **317**, 203–210.

Cashman, P. H. and Ellis, M. A. (1994) Fault interaction may generate multiple slip vectors on a single fault surface. *Geology* **22**, 1123–1126.

Doblas, M. (1985) *SC* deformed rocks: the example of the Sierra de San Vicente sheared granitoids (Sierra de Gredos, Toledo, Spain). A. M. Thesis, Harvard University.

Doblas, M. (1987) Criterios del sentido del movimiento en espejos de fricción: Clasificación y aplicación a los granitos cizallados de la Sierra de San Vicente (Sierra de Gredos). *Estudios Geológicos* **43**, 47–55.

Doblas, M. (1991) Criterios del sentido del movimiento e historia deformativa en fallas a partir de la petrografía de espejos de fricción: Aplicación a fallas alpinas del Sistema Central. *Geogaceta* **10**, 106–109.

Doblas, M. and Oyarzun, R. (1989a) Neogene extensional collapse in the western Mediterranean (Betic-Rif alpine orogenic belt): implications for the genesis of the Gibraltar Arc and magmatic activity. *Geology* **17**, 430–433.

Doblas, M. and Oyarzun, R. (1989b) 'Mantle core complexes' and Neogene extensional detachment tectonics in the western Betic Cordilleras, Spain: an alternative model for the emplacement of the Ronda peridotite. *Earth and Planetary Science Letters* **93**, 76–84.

Doblas, M., Ubanell, A. and Villaseca, C. (1988) Deformed porphyry dikes in the Spanish Central System. *Rendiconti Societa Italiana Mineralogia & Petrologia* **43**, 517–524.

Doblas, M., Mahecha, V., Hoyos, M. and López-Ruiz, J. (1993) High-angle origin of the low-angle Sierra Nevada extensional detachment system: Alpine Betic Cordilleras, southern Spain. *Geological Society America, Abstracts with Programs* A-480.

Doblas, M., Mahecha, V., Hoyos, M., López-Ruiz, J. and Aparicio, A. (1995) Slickenside kinematic indicators in high- and low-angle normal faults in the Alpine Betic cordilleras, southern Spain. *Geological Society America Penrose Conference on 'Fine-grained Fault Rocks'*, Leavenworth, Washington.

Dumont, J. F., Uysal, S. and Simsek, S. (1981) Superposition des jeux sur une faille et succession des événements néotectoniques. L'exemple d'Éphése (Turquic). *Comptes rendus Sommaires Société geologique de France* **1**, 22–24.

Dunne, W. M. and Hancock, P. L. (1994) Palaeostress analysis of small-scale brittle structures. In *Continental Deformation*, ed. P. L. Hancock. Pergamon Press, Oxford, 101–120.

Dzulynski, S. and Kotlarczyk, J. (1965) Tectogliphs on slickensided surfaces. *Bulletin Academy Poland Science* **13**, 149–154.

Engelder, I. T. (1974) Microscopic wear grooves on slickensides: indicators of paloseismicity. *Journal of geophysical Research* **79**, 4387–4392.

Gay, N. C. (1970) The formation of step structures on slickensided shear surfaces. *Journal of Geology* **78**, 523–532.

Guiraud, M. and Séguret, M. (1987) Soft-sediment microfaulting related to compaction within the fluvio–deltaic infill of the Soria strike-slip basin (northern Spain). In *Deformation of Sediments and Sedimentary Rocks*, eds M. E. Jones and R. M. F. Preston. *Special Publication geological Society London* **29**, 123–136.

Gray, M. B. and Nickelsen, R. P. (1989) Pedogenic slickensides: indicators of strain and deformation processes in red bed sequences of the Appalachian foreland. *Geology* **17**, 72–75.

Hancock, P. L. (1985) Brittle microtectonics: principles and practices. *Journal of Structural Geology* **7**, 431–457.

Hancock, P. L. and Barka, A. A. (1987) Kinematic indicators on active normal faults in western Turkey. *Journal of Structural Geology* **9**, 573–584.

Harris Jr., S. E. (1943) Friction cracks and the direction of glacial movement. *Journal of Geology* **51**, 244–258.

Hoyos, M. (1992) Geomorfología y sistemas kársticos entre Nerja y la Playa de la Herradura (Málaga-Granada). *Informe Técnico de Enadimsa*, Madrid.

IGME (1973) *Mapa geológico de Granada-Málaga, nº 83.* Escala 1:200,000, Instituto Geológico y Minero de España (IGME), Madrid.

IGN (1992) *Análisis sismotectónico de la Península* Ibérica, Baleares, y Canarias. Instituto Geográfico Nacional (IGN), Madrid.

Jackson, R. E. and Dunn, D. E. (1974) Experimental sliding friction and cataclasis of foliated rocks. *International Journal of Rock Mechanics and Mineral Science Geological. Abstracts* **11**, 235–249.

Lee, Y. J. (1991) Slickenside petrography: slip-sense indicators and classification. Unpublished M.Sc. Thesis, State University of New York.

Lee, Y. J. and Means, W. D. (1990) Slickenside petrography. *Geological Society America, Abstracts with Programs* A-182.

Lin, S. and Williams, P. F. (1992) The origin of ridge-in-groove slickenside striae and associated steps in an *S–C* mylonite. *Journal of Structural Geology* **14**, 315–321.

Lister, G. S. and Davis, G. A. (1989) The origin of metamorphic core complexes and detachment faults formed during Tertiary continental extension in the northern Colorado River region, U.S.A. *Journal of Structural Geology* **11**, 65–94.

Means, W. D. (1987) A newly recognized type of slickenside striation. *Journal of Structural Geology* **9**, 585–590.

Means, W. D. (1993) Slickensides as paleoseismographs. *Geological Society America, Abstracts with Programs* A115.

Mercier, J. and Vergely, P. (1992) *Tectonique*, Dunod, Paris.

Moore, D. E., Summers, R. and Byerlee, J. D. (1989) Sliding behavior and deformation textures of heated illite gouge. *Journal of Structural Geology* **11**, 329–342.

Nichols, R. L. (1938) Grooved lava. *Journal of Geology* **66**, 601–614.

Norris, D. K. and Barron, K. (1969) Structural analysis of features on natural and artificial faults. In *Research in Tectonics*, eds E. Baer and D. K. Norris. *Geology Survey Paper Canada* **68-52**, 136–167.

Petit, J. P. (1987) Criteria for the sense of movement on fault surfaces in brittle rocks. *Journal of Structural Geology* **9**, 597–608.

Petit, J. P. and Laville, E. (1987) Morphology and microstructures of hydroplastic slickensides in sandstones. In *Deformation of Sediments and Sedimentary Rocks*, eds M. E. Jones and R. M. F. Preston. *Special Publication geological Society London* **29**, 107–121.

Petit, J. P., Proust, F. and Tapponnier, P. (1983) Critères du sens du mouvement sur les miroirs de failles en roches non calcaires. *Bulletin de la Société geologique de France* **7**, 589–608.

Pierce, W. G., Nelson, W. H., Tokarski, A. K. and Piekarska, E. (1991) Heart Mountain, Wyoming, detachment lineations: Are they in microbreccia or in volcanic tuff? *Bulletin geological Society America* **103**, 1133–1145.

Pollard, D. D., Saltzer, S. D. and Rubin, A. M. (1993) Stress inversion methods: are they based on faulty assumptions? *Journal of Structural Geology* **15**, 1045–1054.

Power, W. L. and Tullis, T. E. (1989) The relationship between slickenside surfaces in fine grained quartz and the seismic cycle. *Journal of Structural Geology* **11**, 879–893.

Ramsay, J. G. and Huber, M. I. (1987) *The Techniques of Modern Structural Geology, Volume 2: Folds and Fractures.* Academic Press, London.

Riecker, R. E. (1965) Fault-plane features: an alternative explanation. *Journal of Sedimentary Petrology* **35**, 746–748.

Rutter, E. H. (1993) The mechanics of natural rock deformation. In *Comprehensive Rock Engineering (Principles, Practice and Projects). Volume 1: Fundamentals*, eds L. A. Hudson, E. T. Brown, C. Fairhust and E. Hoek. Pergamon Press, Oxford, 63–92.

Scholz, C. M. N. (1990) *The Mechanics of Earthquakes and Faulting.* Cambridge University, Cambridge Press.

Sellier, D. and Bossière, G. (1993) Apport de la microscopic électronique à balayage à l'analyse des surfaces d'abrasion glaciaire sur les roches quartzitiques. *Zeitschrift für Geomorphologie N. F.* **37**, 477–499.

Sibson, R. H. (1986) Earthquakes and rock deformation in crustal fault zones. *Annual Review Earth and Planetary Science* **14**, 149–175.

Smith, E. I. (1968) Criteria for the determination of flow direction in volcanic rocks. Unpublished M.Sc. Thesis, University of New Mexico.

Spray, J. G. (1989) Slickenside formation by surface melting during the mechanical excavation of rock. *Journal of Structural Geology* **11**, 895–905.

Stewart, I. S. and Hancock, P. L. (1991) Scales of structural heterogeneity within neotectonic normal fault zones in the Aegean region. *Journal of Structural Geology* **13**, 191–204.

Suppe, J. (1985) *Principles of Structural Geology.* Prentice Hall, Englewood Cliffs, New Jersey.

Suter, M., Martinez, M. C., Martinez, M. L. and Farrar, E. (1995) The Aljibes half-graben: Active extension at the boundary between the trans-Mexican volcanic belt and the Basin and Range province, Mexico. *Bulletin geological Society America* **107**, 627–641.

Torres-Roldán, R. L. (1979) The tectonic subdivision of the Betic Zone (Betic cordilleras, southern Spain): its significance and one possible geotectonic scenario for the westernmost alpine belt. *American Journal Science* **279**, 19–51.

Tjia, H. D. (1967) Sense of fault displacements. *Geologie en Mijnbouw* **46**, 392–396.

Tjia, H. D. (1968) Fault-plane markings. *XXIII International Geological Congress* **13**, 279–284.

Tullis, T. E. (1993). The difficulty of determining whether slip on an ancient fault was seismic or not. *Geological Society America, Abstracts with Programs* A114.

Vialon, P., Ruhland, M. and Grolier, J. 1976. *Eléments de Téctonique Analytique.* Masson, Paris.

Wardlaw, N. C., Stauffer, M. R. and Hoque, M. (1969) Striations, giant grooves, and superposed drag folds, Interlake area, Manitoba. *Canadian Journal of Earth Science* **6**, 577–593.

Will, T. M. and Wilson, C. J. L. (1989) Experimentally produced slickenside lineations in pyrophyllitic clay. *Journal of Structural Geology* **11**, 657–667.

Willis, B. and Willis, R. (1934) *Geologic Structures.* McGraw-Hill, New York.

Wilson, C. J. L. and Will, T. M. (1990) Slickenside lineations due to ductile processes. In *Deformation Mechanisms, Rheology and Tectonics*, eds R. J. Knipe and E. H. Rutter. *Special Publication geological Society London* **54**, 455–460.